frontiers | Frontiers in Earth Science

TYPE Original Research
PUBLISHED 17 January 2023
DOI 10.3389/feart.2022.1071466

OPEN ACCESS

EDITED BY
Tao Hu,
China University of Petroleum, China

REVIEWED BY
Di Chen,
China University of Petroleum, China
Li Ang,
Jilin University, China

*CORRESPONDENCE
Longlong Li,
lilonglongyx@126.com

SPECIALTY SECTION
This article was submitted to Geochemistry, a section of the journal Frontiers in Earth Science

RECEIVED 16 October 2022
ACCEPTED 11 November 2022
PUBLISHED 17 January 2023

CITATION
Peng J, Li L, Du C, Liu X, Zhu J, Liang S, Qiu Q and Wang D (2023), Hydrocarbon generation and expulsion modeling of different lithological combination source rocks from the Funing Formation in the Subei Basin.
Front. Earth Sci. 10:1071466.
doi: 10.3389/feart.2022.1071466

Hydrocarbon generation and expulsion modeling of different lithological combination source rocks from the Funing Formation in the Subei Basin

Jinning Peng[1,2], Longlong Li[1,2]*, Chongjiao Du[1,2], Xu Liu[1,2], Jianhui Zhu[1,2], Shiyou Liang[1,2], Qi Qiu[1,2] and Dongyan Wang[1,2]

[1]Wuxi Research Institute of Petroleum Geology, SINOPEC Petroleum Exploration and Production Research Institute, Wuxi, China, [2]State Key Laboratory of Shale Oil and Gas Enrichment Mechanisms and Effective Development, Wuxi, China

The oil expulsion efficiency and retention efficiency of shale affect the enrichment and preservation of shale oil. Two series of semi-closed hydrous pyrolysis experiments were performed under *in situ* geological conditions on a Paleogene shale sample as a comparable analog to evaluate the generation and preservation potential of shale oil in the Funing Formation shale in the Subei Basin. The results show that 1) the oil-generation capacity evolution of different lithological combination source rocks in the Funing Formation of the Subei Basin can be roughly divided into four stages: a) relatively slow oil-generating and slow gas-generating, b) relatively fast oil-generating and slow gas-generating, c) oil cracking into gas, and d) kerogen cracking into gas; 2) different lithological combinations have different hydrocarbon generation, expulsion, and retention efficiencies. The total oil generation rate and gas generation rate of pure shale are higher than those of shale with a silty interlayer, and the exchange point between the oil expulsion rate and retention rate of pure shale is earlier than that of shale with the silty interlayer, which indicates that the pure shale experienced the expulsion and retention process earlier. Oil retention mainly occurs at an EqVRo of 0.84%–1.12%, while oil is mainly discharged to the adjacent siltstone at an EqVRo of 1.12%–1.28%. Based on the simulation under geological conditions, it is recognized that for shale oil exploration in the Subei Basin, the favorable thermal maturity is at an EqVRo of 0.84%–1.12%, and the favorable lithology is the shale with the silty interlayer. On one hand, the siltstone interlayer can provide pore space for the early generated oil, and the concentration difference of hydrocarbons between the shale and the interlayer can be formed so that the generated shale can continuously enter the interlayer. On the other hand, the shale above the interlayer can be used as a cap rock to preserve shale oil. The favorable area for shale oil exploration in the Subei Basin is the area with relatively high maturity (at a VR value of about 1.1%)

KEYWORDS

shale oil, lacustrine shale, hydrocarbon generation and expulsion, modeling, Subei Basin

1 Introduction

The successful exploration and production of Chang 7 shale oil in the Ordos Basin and the Lucaogou shale oil in the Junggar Basin have made scholars realize the promising prospective of lacustrine shale oil worldwide (Jia et al., 2012; Yang et al., 2017; Hu et al., 2018; Hou et al., 2021a; Hu et al., 2021; Jin et al., 2021; Wang et al., 2022). In 2021, the wells SD1, QY1-HF, and SY3-7HF, were drilled into the Funing Formation in the Subei Basin and harvested high oil flow reaching industrial production levels with a proven reserve exceeding 3.5 $\times 10^9$ t, making the Funing Formation another important target for shale oil exploration in China (Yao et al., 2021).

The second member (E_1f^2) and fourth member (E_1f^4) of the Paleogene Funing Formation in the Subei Basin, with abundant shale oil sources, have been highly valued. These source rocks are characterized by a medium degree of thermal maturation and TOC, good organic matter type, large thickness, and wide distribution, which provide material conditions for the occurrence and enrichment of shale oil (Ji et al., 2013). Many previous works have been conducted on organic and inorganic geochemical characteristics, sedimentary environment, physical properties, and fractures of the Funing shale in the Subei Basin (Zhang et al., 2003; Quaye et al., 2018; Cheng et al., 2019; Liu et al., 2020; Peng et al., 2020). Meanwhile, many favorable areas of shale oil exploration were proposed and implemented (Zan et al., 2021a).

However, little interest has been paid to hydrocarbon generation and expulsion at the different stages of thermal maturity for the Funing shale, which is a key issue in shale oil exploration. Significant progress has been made in the study of hydrocarbon generation and expulsion of other lacustrine shales, but they cannot directly apply to the Funing shale, which is due to its strong heterogeneity and variation in large sedimentary facies (Anyiam and Onuoha, 2014; Shi et al., 2018; Tang et al., 2018; Ma et al., 2020). The Funing shale often contains thin siltstone and a carbonate interlayer, which may have a potential impact on hydrocarbon generation and expulsion. Therefore, a detailed analysis is crucial to the hydrocarbon generation and expulsion of organic-rich shales in the Funing Formation.

Pyrolysis experiments are important methods to understand the formation and evolution processes of oil and gas (Mahlstedt and Horsfield, 2012; Uguna et al., 2016). Pyrolysis experiments have been conducted to investigate the influences of the oil expulsion efficiency on shale gas generation and occurrence (Hill et al., 2007; Jia et al., 2014; Ma et al., 2021). Hydrocarbon generation simulation experiments are of three types: open system, closed system, and semi-closed system (Hu et al., 2022). The open-system experiment is widely used because of its fast economy and real-time and online measurement of products, but it is difficult to obtain an intuitive relationship between the hydrocarbon generation rate and maturity, which has also been questioned by some scholars when applied to geological conditions (Qin et al., 2011). The closed system can not only simulate the oil generation of source rocks in different thermal evolution stages but also simulate the maximum gas generation (Lu et al., 2006), while the semi-closed system hydrous pyrolysis is supposed to be more closed to natural underground geological conditions, better than the closed-system pyrolysis in which generated petroleum cannot be expelled and consequently cracks into gaseous hydrocarbon, causing less oil to be generated than in natural conditions, and better than the open system in which generated hydrocarbons were fully expelled out and allow the reaction of hydrocarbon generation stay the course, leading to production and expulsion of more hydrocarbons than in natural conditions (Tang et al., 2015).

In this study, a semi-closed hydrous pyrolysis system was used to investigate the generation, which has proven to be a reliable instrument for investigation of hydrocarbon generation, retention, and expulsion (Zheng et al., 2009; Ma et al., 2017). In this study, by using DK-III, hydrocarbon generation, retention, and expulsion of two different lithological combinations from the E_1f^2 and E_1f^4 were investigated with increasing thermal maturity. This work may provide a comparable measure to evaluate shale gas generation, retention, and expulsion for low-thermal maturity lacustrine shales and also provide some suggestions for shale oil exploration in the Subei Basin.

2 Geological settings

The Subei Basin is in the land part of the South Yellow Sea Basin. It is a composite basin superimposed by multiple stages and types of basins (Shu et al., 2005; Qi et al., 2018). The basin is bounded by the Binhai Uplift in the north, Southern Jiangsu Uplift in the south, Shandong–Jiangsu Uplift in the west, and the Yellow Sea in the east (Figure 1). The basin has undergone multiple tectonic movements and transformation and is divided into Yanfu Depression, Jianhu Uplift, and Dongtai Depression from north to south (Chai, 2019). The study area (Jinhu Sag) is in the western part of the Dongtai Depression (Figure 1). The base in the Subei Basin is marine Paleozoic–Mesozoic deposits, and the caprock is a continental Mesozoic–Cenozoic fault depression sedimentary body, including Taizhou Formation (K_2t), Funing Formation (E_1f), Dainan Formation (E_2d), Yancheng Formation (N_2y), and other sets of strata (Shi, 2010). The thickness of Mesozoic–Cenozoic deposits is over 11,000 m.

The E_1f was deposited in the basin depression evolution stage, widely distributed in different structural parts of various depressions (Zan et al., 2021b). The thickness of E_1f is over 7,000 m including the four members (E_1f^1–E_1f^4) from the bottom to the top. The E_1f^1 and E_1f^3 consist of a set of fluvial deltaic sandstone and siltstone, while the E_1f^2 and E_1f^4 were deposited in the lacustrine and dark lake mudstone and shale are important source rock sections (Duan et al., 2020; Liu et al., 2020). The E_1f

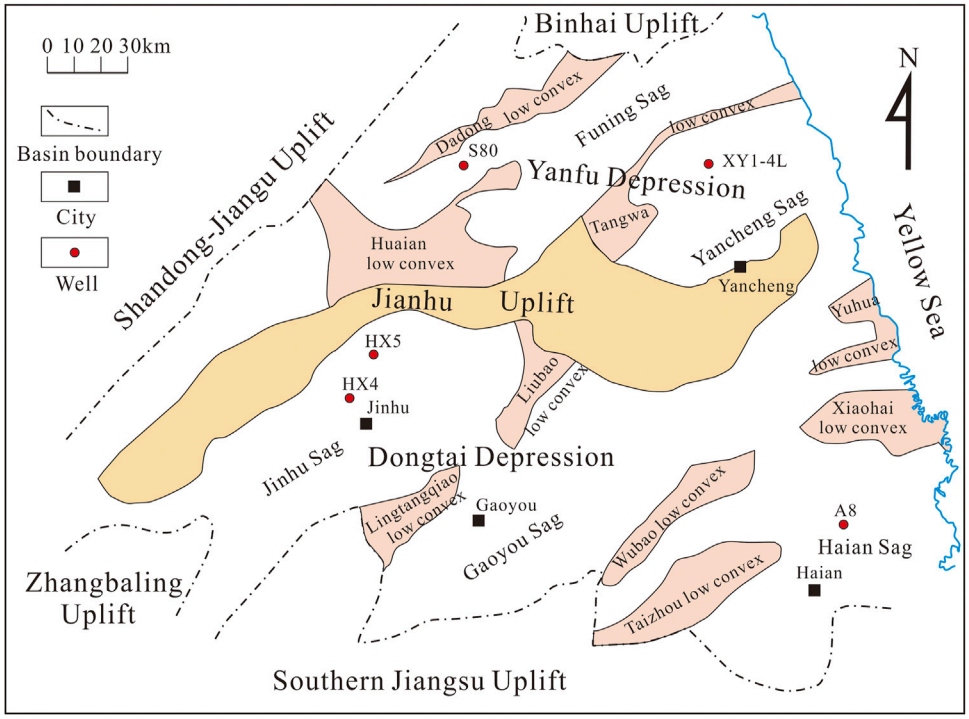

FIGURE 1
Geological setting of the Subei Basin.

was not further buried until the end of Yancheng Formation sedimentation due to the two stages of uplift and denudation, and source rocks began to enter the oil window (Liu, 2010). At present, the source rock in the E_1f^2 has reached high thermal maturity in the deep depression zone of the Subei Basin, while its maturity is lower in the slope and low uplift (Zhao et al., 2022). The thermal maturity of the source rock in the E_1f^4 is still lower owing to the shallow burial depth (Liu, 2010).

3 Samples and methods

3.1 Samples

For the pyrolysis simulation of hydrocarbon generation, the samples of immature to low-mature source rock are more representative (Ma et al., 2021). To investigate the typical hydrocarbon generation and expulsion processes of source rocks from the E_1f^2 and E_1f^4 in the Subei Basin, two samples were selected from the E_1f^2 and E_1f^4 to be prepared for the experiments according to fundamental geochemical analysis data. The total organic carbon content was detected using a carbon sulfur analyzer (CS-230) according to the Chinese standard GB/T 19145–2003 (GB/T 19145-2003, 2003); the hydrogen index and maximum pyrolysis temperature were tested using a Rock-Eval analysis; and the vitrinite reflectance (VR) was analyzed according to the Chinese standard GB/T 6948–2008 (GB/T 6948-2008, 2008).

3.2 Semi-closed hydrous pyrolysis system

Two samples are prepared to experiment different lithology combinations. Considering the fact that shale often contains silty sand and a sandy interlayer in the actual geological conditions of the Subei Basin, we designed two models to simulate the hydrocarbon generation and expulsion characteristics of shale with a silty interlayer (model 1) and pure shale (model 2).

Experiments were carried out using a high-temperature and high-pressure semi-closed hydrous pyrolysis system. The instrument is capable of conducting pyrolysis experiments under *in situ* geological conditions. It is mainly composed of a high-temperature and high-pressure reaction system, a two-way hydraulic control system, an automatic hydrocarbon expulsion product collection and fluid supplement system, a data acquisition and automatic control system, and peripheral auxiliary equipment.

The simulation experiment of hydrocarbon generation and expulsion of source rock with this instrument has the following characteristics: 1) the original cylinder sample with a diameter of

TABLE 1 Hydrocarbon generation and expulsion experiment program of source rock sample HX4 in the Jinhu Sag, Subei Basin.

Simulation temperature (°C)	Simulation time (h)	Fluid pressure (Mpa)	Static rock pressure (Mpa)	Weight of source rock (g)	Weight of overlying sandstone (g)	Weight of underlying sandstone (g)
250	48	20	36.8	60.98	20.14	20.6
275	48	21.5	39.1	60.1	20.54	20.39
300	48	23.8	43.7	60.75	20.9	20.11
310	48	25	46	60.55	20.7	20.39
320	48	27.5	50.6	59.14	20.19	20.41
335	48	30	55.2	58.28	20.72	20.36
350	48	32.5	59.8	59.85	20.27	20.15
360	48	35	64.4	59.48	20.21	20.56
370	48	40	73.6	58.6	20.96	20.55
380	48	43.8	80.5	60.32	20.78	20.71
400	48	50	92	60.49	20.48	20.36

3.8 cm and a mass of 5–150 g is drilled using a special sampling tool, and the original pore structure, composition, and organic matter occurrence state of the sample are retained as much as possible; 2) the original cylinder is sealed in the sample chamber as a whole and placed in a high-temperature autoclave. Then, the core sample is compacted by applying a static rock pressure up to 180 MPa through the oil cylinder and the middle pressure sleeve. Only a pipe with a very small inner diameter is connected with the automatic hydrocarbon expulsion product collection system. Therefore, the closed simulation of the hydrocarbon generation process is carried out in the rock pore space with almost no spare reaction space; 3) the original pore fluid of the cylinder in the sample chamber (which can supplement both formation of water and inert gas) can be supplemented in real-time through the fluid supplement system. The port of the autoclave body adopts a special sealing method combining axial self-tight static sealing and semi self-tight dynamic sealing. Therefore, the high-pressure hydrocarbon generation and expulsion simulation experiment can be conducted under the condition that the maximum pore fluid pressure reaches 150 MPa; and 4) the high-pressure valve is automatically controlled by hydrocarbon expulsion, so it can not only simulate closed hydrocarbon generation under a certain pore fluid pressure but also simulate "episodic hydrocarbon expulsion" under a higher fluid pressure. Key parameters of the instrument are introduced by Zheng et al. (2009) in detail.

3.3 Experimental procedure

According to the reconstructed burial history of the Funing Formation in the Subei Basin (Liu, 2019), the fluid pressure and static rock pressure were set (Table 1). The Funing Formation shale underwent a short-term burial before reaching a maximum depth of 3,200 m at 38 Ma and an EqVRo <1.0% (Liu, 2019). In this study, EqVRo values corresponding to different experimental temperatures were obtained from the pyrolysis experiments of immature coal samples (Table 1). The experimental temperatures were increased at a heating rate of 1°C/min and were maintained at the final temperature for 48 h. For two models, the experiment process is shown in Figure 2 and Figure 3, and experiment conditions are listed in Table 1 and Table 2.

The specific experiment steps are as follows:

1) To ensure that each temperature point simulating the experimental source rock is consistent to reduce the experimental error, the sample was crushed to the specified size (60 mesh) and divided into 11 equal parts, each about 60 g. After that, 11 small cylindrical core samples of siltstone (3.5 cm in diameter) were prepared. For model 1, the gray siltstone sample of well HX4 (2,357.6 m depth) was crushed to the same size (60 mesh); after chloroform extraction, hydrogen peroxide and other reagents are used to remove organic matter and dried. The samples are divided into 22 equal parts, and a small core sample of siltstone cylinder with a diameter of 35 mm is also prepared. Then, the prepared siltstone small cylinders, shale small cylinders, and siltstone small cylinders are loaded into the sample chamber in sequence, and the small cylinders are separated using filters (see Figure 2). For model 2, similarly, the pure shale sample XY1 is crushed to the specified size (60 meshes) and divided it into 11 equal parts, about 60 g each. The instrument is used to make a uniform-sized cylinder core sample of pure shale hydrocarbon source rock (with a diameter of 3.5 cm).
2) When the sample was loaded, a series of leak tests were performed. Helium gas was injected with a pressure of 8 MPa. This process is repeated five–six times to ensure that the reaction device is sealed and airtight.

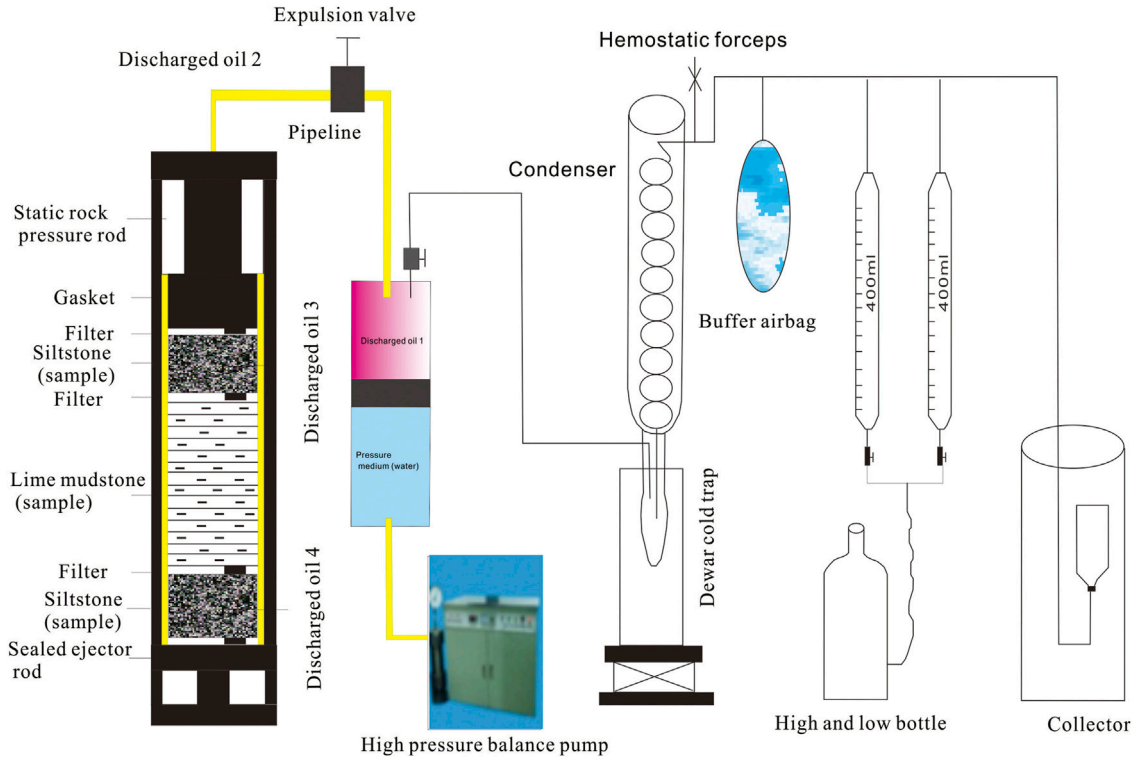

FIGURE 2
Hydrous pyrolysis system for hydrocarbon generation and expulsion of shale with a silty interlayer (model 1).

3) Distilled water was injected into the reactor with high pressure. Then, pressure is applied and the sample is heated: the two-way hydraulic press is used to apply static rock pressure to the pressure value corresponding to each temperature point through the static rock pressure rod, and then the temperature control device is used to increase the set temperature at a rate of 1°C/min, and the temperature is maintained after reaching the set temperature for 2 days (48 h). It should be noted that during the experiment, the fluid pressure in the reaction device will continue to increase as the argillaceous source rock generates hydrocarbons continually. At this time, when the fluid pressure exceeds the set hydrocarbon expulsion pressure, the hydrocarbon expulsion valve is adjusted (Figure 3) to make the fluid pressure in the reaction device consistent with the pressure of the external hydrocarbon expulsion device and it is maintained at the set pressure value.
4) After the completion of each set of simulation experiments, the discharge oil collection and quantitative research are carried out after the oil, gas, and water products in the simulation device are discharged.
5) Finally, after the experiment, the maturity analysis of the shale residual samples after the 11 groups of formation pore thermal pressure generation, expulsion, and retention of hydrocarbons is used to determine the maturity of the shale corresponding to the source rock under 11 different temperature and pressure conditions. According to Burnham's 1989 type II kerogen, the relationship between temperature and maturity was calculated using an EasyRo model (Burnhan and Sweeney, 1989).

3.4 Product analysis

Due to the different lithologies of the model settings, the products of the two models have different geological significances. For model 1, according to the simulation program of the lithological combination of shale with the silty interlayer, "discharged oil 1" shown in Figure 2 is the oil discharged due to the pressure difference between the hydrocarbon generation system and the hydrocarbon expulsion system in the experimental device, which can be regarded as a simulation of real geological conditions (the oil generated by the source rock from the source layer is discharged from the source rock through the migration channel to the oil accumulated in the reservoir outside the source layer); "discharged oil 2" refers to the oil generated from the shale discharged to the inner wall of the sample reaction device and the

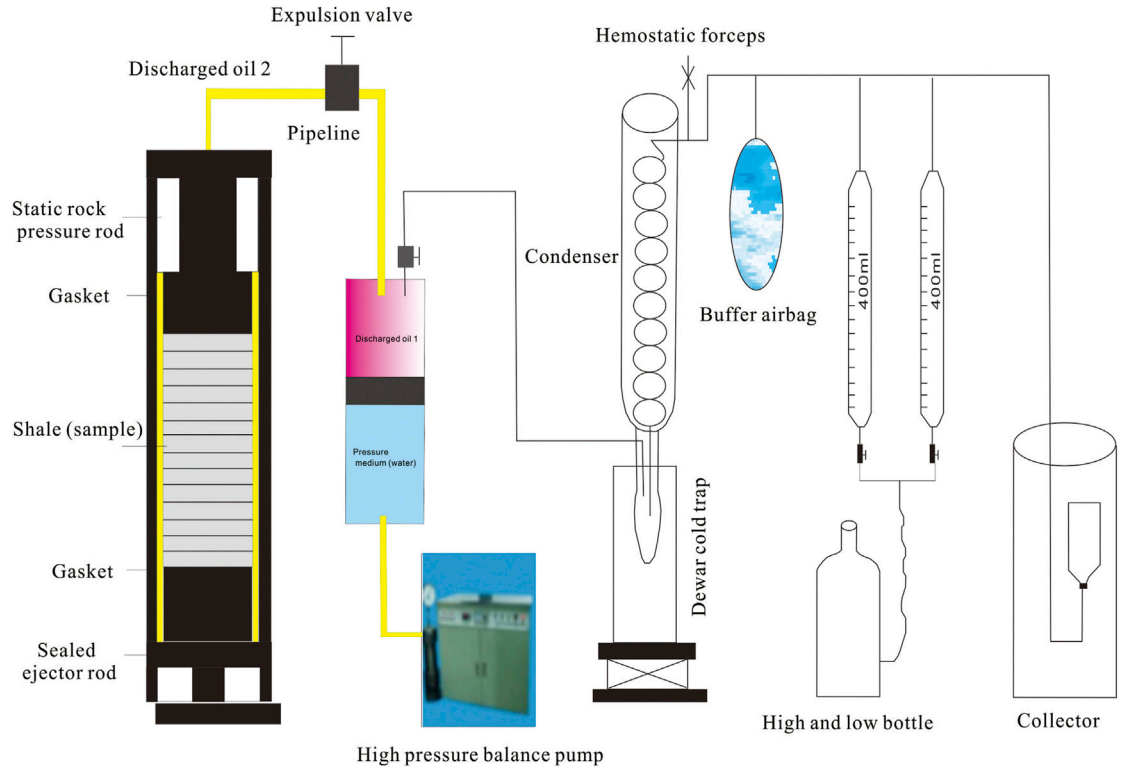

FIGURE 3
Hydrous pyrolysis system for hydrocarbon generation and expulsion of pure shale (model 2).

TABLE 2 Hydrocarbon generation and expulsion experiment program of source rock sample no. XY1-4L in the Yancheng Sag, Subei Basin.

Simulation temperature (°C)	Simulation time (h)	Fluid pressure (Mpa)	Static rock pressure (Mpa)	Weight of source rock (g)
250	48	22.1	51	60.10
275	48	26.3	60	60.10
300	48	27.9	64	60.50
325	48	30.4	70	60.18
350	48	34.1	78	60.11
375	48	36.7	84	60.00
400	48	39.3	90	59.95
425	48	41.2	95	59.63
450	48	43.5	100	58.34
475	48	47.7	110	57.79
500	48	51.9	119	60.40

inside of the dredging pipeline, which can be regarded as the oil discharged into the migration channel such as cracks under simulated real geological conditions. “Discharged oil 3” and “discharged oil 4” refer to the oil generated from the shale source rock being discharged to the core powder placed up and down due to the difference between the shale source rock and siltstone cores placed above and below. It can be regarded as the shale source rock migrated and accumulated in the siltstone in a short distance after rupture and hydrocarbon expulsion under the simulated real geological conditions. Residual oil

TABLE 3 Geochemical characterization of source rock samples used for pyrolysis.

Sample no.	Lithology	Depth (m)	Layer	S_1 mg/g	S_2 mg/g	Tmax (°C)	TOC (%)	HI mg/g	Ro (%)
HX4	Shale with a silty interlayer	1,896.3	E_1f^4	0.04	11.46	438	2.13	538	0.57
XY1-4L	Gray shale	1,613.5	E_1f^2	0.64	25.60	433	4.65	551	0.54

E_1f^4, the fourth member of the Funing Formation; E_1f^2, the second member of the Funing Formation; S_1, amount of free hydrocarbons; S_2, amount of pyrolysis hydrocarbons; Tmax, TOC, total organic carbon; HI, hydrogen index; Ro, vitrinite reflectance.

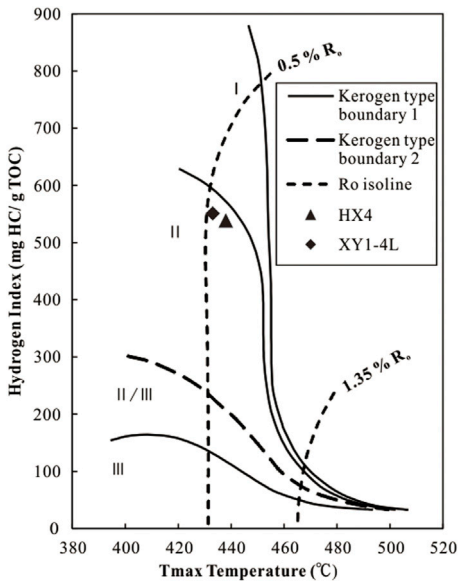

FIGURE 4
Kerogen type classification chart.

(retained oil) refers to the oil remaining in the shale source rock (existing in a free, adsorbed, and mutually soluble state) after simulation and usually refers to the bitumen "A" obtained by chloroform extraction. The total oil usually refers to the sum of the residual oil and the aforementioned discharged oil, and the total hydrocarbon usually refers to the sum of the total oil and hydrocarbon gas. Model 2 has three parts of oil and hydrocarbon gas: "discharged oil 1," "discharged oil 2," and residual oil (retained oil) (Figure 3).

4 Results

4.1 Evaluation of the geochemical parameters

Geochemical characteristics of these two samples are given in Table 3. The samples are organic-rich, low-mature, and contain type I kerogen. Total organic carbon (TOC) contents for the samples are 2.13% (HX4) and 4.65% (XY1-4L), with a hydrogen index of 538 and 551 mg HC/g TOC, respectively (Table 3). The two samples are low-mature (Ro<0.6%), and the organic matter is kerogen type II according to the Rock-Eval analysis (Figure 4) (Mukhopadhyay et al., 1995).

4.2 Oil products of model 1

4.2.1 Retained oil

The retained oil of model 1 is given in Table 4 and shown in Figure 5A. The retained oil reaches a peak of 333.53 mg/g TOC at an EqVRo of 0.84%, and there is no retained oil observed until an EqVRo of 2.0%.

4.2.2 Discharged oil

The discharged oil of model 1 is given in Table 4 and shown in Figure 5B. When the EqVRo is less than 0.74%, there is no discharged oil. With the increase in temperature, the amount of discharged oil gradually increases until Ro=1.28, reaching a maximum of 409.36 mg/g TOC; the yields then rapidly decrease to 342.1 mg/g TOC at 2.0% of EqVRo. In addition, the discharged oil consists of four parts as shown in Figure 5B. This discharged oil increased with temperature, especially discharged oil 1, and it reaches 206.49 mg/g TOC at 2.0% of EqVRo as same as discharged oil 2 of 75.27 mg/g TOC. However, discharged oils 3 and 4 form a trend of increasing first and then decreasing at 1.12% and 0.84% of EqVRo, respectively.

4.2.3 Total hydrocarbon

The hydrocarbons of model 1 are given in Table 4 and shown in Figure 5C. Before the EqVRo reaches 0.8%, the total hydrocarbon contains almost only oil with a value of 409.4 mg/g TOC. When the EqVRo reaches 1.28%, the oil yield is the highest and oil begins to crack into gas.

4.3 Oil products of model 2

4.3.1 Oil yields

The oil yields of model 2 are given in Table 5 and shown in Figure 6A. The oil yields reach the maximum 625.83 mg/g TOC

TABLE 4 Retained and discharged oil yields of model 1.

Sample	Temperature (°C)	EqVRo (%)	Oil yields (mg/g TOC)				Discharged oil (mg/g TOC)				Total hydrocarbon (mg/g TOC)		
			Total oil	Retained oil	Discharged oil	Discharged oil 1	Discharged oil 2	Discharged oil 3	Discharged oil 4	Total discharged oil	Total hydrocarbon	Total oil	Total gas
HX4-1	250	0.59	83.28	76.68	6.61	1.54	3.53	0.00	1.54	6.61	91.76	83.28	8.47
HX4-2	275	0.64	137.67	119.11	18.56	5.52	7.52	0.00	5.52	18.56	148.49	137.67	10.82
HX4-3	300	0.68	171.79	155.67	16.12	5.52	5.52	1.54	3.53	16.12	182.61	171.79	10.82
HX4-4	310	0.7	218.21	198.10	20.10	11.50	3.53	1.54	3.53	20.10	226.68	218.21	8.47
HX4-5	320	0.74	270.10	226.09	44.01	19.47	11.50	5.52	7.52	44.01	290.31	270.10	20.20
HX4-6	335	0.8	396.23	350.23	46.01	27.44	9.51	5.52	3.53	46.01	409.40	396.23	13.17
HX4-7	350	0.84	518.44	372.80	145.64	31.43	5.52	33.42	75.27	145.64	540.99	518.44	22.55
HX4-8	360	0.9	517.03	333.53	183.50	33.42	5.52	91.21	53.35	183.50	544.27	517.03	27.24
HX4-9	370	1.12	503.09	217.97	285.13	95.19	5.52	119.11	65.30	285.13	549.10	503.09	46.01
HX4-10	380	1.28	515.22	110.53	404.69	164.94	37.41	73.27	129.07	404.69	575.31	515.22	60.08
HX4-11	400	2	349.78	14.83	334.95	206.79	75.27	15.49	37.41	334.95	501.36	349.78	151.58

10.3389/feart.2022.1071466

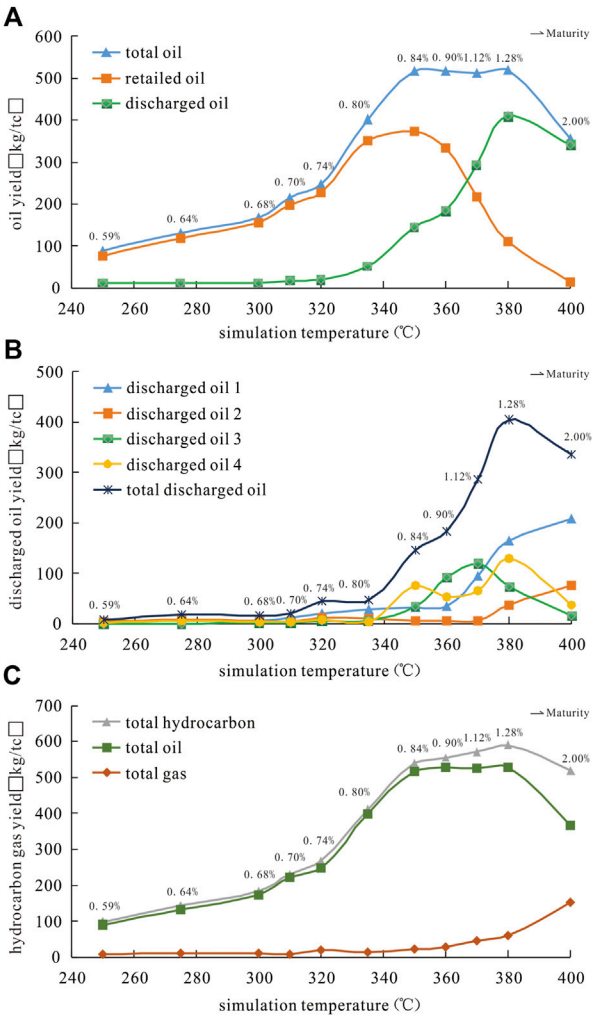

FIGURE 5
Oil yields **(A)**, discharged oil yields **(B)**, and hydrocarbon gas yields **(C)** of shale with a silty interlayer (model 1).

at an EqVRo of 0.8% as well as the discharged oil of 497.7 mg/g TOC.

4.3.2 Gas yields

The gas yields of model 2 are given in Table 5 and shown in Figure 6B. The gas yields begin to increase after an EqVRo of 0.8% and then increases quickly after an EqVRo of 1.61%, with the maximum value of 480.19 mg/g TOC at an EqVRo of 3.08%.

4.4 Stages of shale oil generation

According to the aforementioned experiments, under different temperature and pressure conditions (different thermal evolution stages), the productivity characteristics of oil generation and hydrocarbon generation, oil expulsion, and residual oil (retained oil) of lacustrine shale in the Subei Basin have a clear change rule. It can be seen that with the increase in temperature and pressure in the 11 simulation settings, the thermal evolution degree of organic matter in the source rock in the geological period increases, and the change characteristics of the discharged oil, residual oil (retained oil), and hydrocarbon gas yield of this type of source rock have gone through four stages, shown as follows.

4.4.1 Shale with a siltstone interlayer

In the first stage, the maturity of organic matter Ro increases from 0.59% to 0.74%: this is a stage of slow oil generation and a small amount of gas generation for shale with silty intercalation, and the total oil and gas yield increases slowly with the increase of maturity. At the same time, the oil discharge rate of this type is very low during this period, and the main part of the generated oil is still retained in the source rock: when Ro=0.59%, it can be seen from the total oil discharge that the oil discharged is mainly "discharged oil 1" and "discharged oil 3." When Ro=0.74%, the oil discharge rate and the oil retained (residual oil) rate are slightly increased, but the oil discharge rate is basically unchanged. The expulsion of oil is still dominated by "discharged oil 1" and " discharged oil 3," which indicates that when the evolution degree is low, the hydrocarbon source rock is mainly detained in the rock, and the main favorable expulsion direction is the upper reservoir, and the downward expulsion of the hydrocarbon source rock is basically not possible.

In the second stage, the maturity of organic matter Ro increases from 0.74% to 0.84%: this is the stage of rapid oil generation and slow hydrocarbon generation of silty intercalated shale. The total oil yield increases rapidly with the increase of maturity, but the gas yield does not change significantly, showing a slow increase. When Ro=0.80%, the discharged oil is mainly "discharged oil 1" and "discharged oil 2." However, when Ro=0.84%, the total oil yield and gas yield increase rapidly, approaching the maximum value, and the oil yield and oil discharge rate in this stage increase significantly compared with the previous stage. At this time, the proportion of discharged oil is dominated by "discharged oil 4," "discharged oil 3," and "discharged oil 1," which indicates that when the evolution degree is moderate, the source rock itself is basically saturated, and the favorable direction of hydrocarbon expulsion is to discharge to the upper part and permeate downward.

In the third stage, the maturity of organic matter Ro increases from 0.84% to 1.28%: in this stage, the amount of oil generated by the silty intercalated shale is small, and the total oil yield does not change with the increase of maturity, which is generally maintained at the level equivalent to the total oil yield value at 0.84% maturity, presenting an almost stable platform. At this stage, the gas generation capacity is significantly enhanced. When Ro=1.28%, the gas yield increases rapidly. At the same time, the

TABLE 5 Retained and discharged oil yields of model 2.

Sample	Temperature (°C)	EqVRo (%)	Oil yield (mg/g TOC)			Total hydrocarbon (mg/g TOC)		
			Discharged oil yield	Retained oil yield	Total oil yield	Hydrocarbon gas yield	Total oil yield	Total hydrocarbon yield
XY1-1	250	0.59	8.67	152.01	160.68	4.26	160.68	164.94
XY1-2	275	0.64	4.93	199.79	204.71	13.98	204.71	218.70
XY1-3	300	0.68	40.53	275.20	315.73	9.41	315.73	325.14
XY1-4	325	0.75	171.68	275.20	446.89	38.58	446.89	485.47
XY1-5	350	0.8	497.70	128.12	625.83	52.88	625.83	678.71
XY1-6	375	1.13	315.02	123.90	438.93	125.53	438.93	564.45
XY1-7	400	1.61	418.07	16.64	434.71	164.43	434.71	599.14
XY1-8	425	2.03	386.69	0.71	387.40	164.43	387.40	551.83
XY1-9	450	2.51	354.84	4.93	359.76	276.55	359.76	636.31
XY1-10	475	2.75	402.62	0.00	402.62	353.77	402.62	756.39
XY1-11	500	3.08	362.80	0.00	362.80	480.19	362.80	842.99

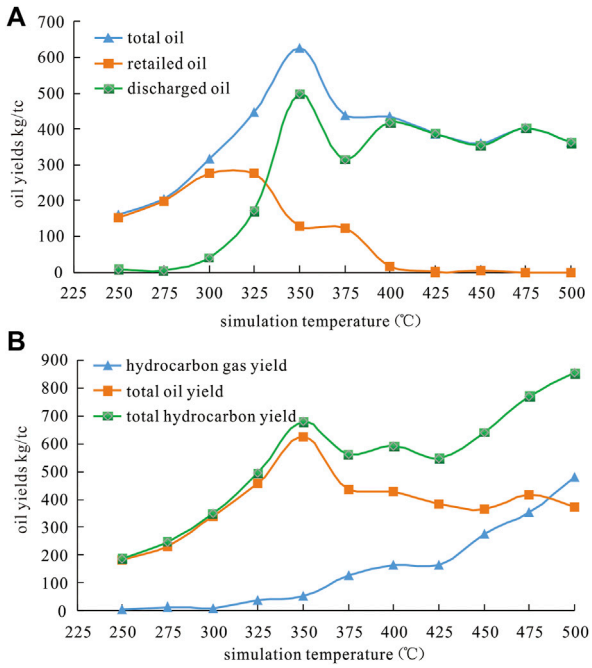

FIGURE 6
Oil yields **(A)** and hydrocarbon yields **(B)** of pure shale (model 2).

yield and rate of oil discharged in this stage increase rapidly. When Ro=1.28%, the oil discharged is dominated by "discharged oil 1," "discharged oil 4," and "discharged oil 3," which indicates that the generated oil may be lifted by gas after it starts to generate gas so that the oil in the whole system will be discharged to the upper part.

In the fourth stage, the maturity Ro > 1.28%: in this stage, the total oil yield, the output oil yield, and the residual oil yield of the silty intercalated shale decrease rapidly, while the gas yield increases rapidly. It shows that the evolution degree of organic matter Ro is more than 2.00%, and the oil generated from the source rock and the discharged oil begin to crack into gas. When Ro=2.00%, the oil drainage rate is very high, and "discharged oil 1" and "discharged oil 2" are the main ones. This shows that the oil in the source rock and its interlayer are discharged rapidly due to the expansion of generated gas, which is similar to the early high production but rapid decline characteristics of shale oil wells in high-maturity areas.

4.4.2 Pure shale

In the first stage, the maturity of organic matter Ro increases from 0.59% to 0.68%: in this stage, the pure shale generates oil slowly and will not generate gas basically. The total oil yield increases slowly with the increase of maturity, while the gas yield changes little with the increase of maturity. The yield of discharged oil in this stage is very low.

In the second stage, the maturity of organic matter Ro increases from 0.68% to 0.84%: in the stage of rapid oil generation and slow gas generation of pure shale, the total oil yield increases significantly with the increase of maturity, while the gas yield increases slowly and the output oil yield also increases rapidly in this stage.

In the third stage, the maturity of organic matter Ro increased from 0.84% to 2.00%: in this stage, the generated oil of pure shale began to crack into gas and the yield of residual oil and discharged oil decreased with the increase of maturity, while the gas yield increased significantly.

In the fourth stage, the maturity of organic matter Ro is 2.00%: in this stage, a large amount of oil generated from pure shale is cracked into gas and a large amount of kerogen is generated. With the increase of simulation temperature, the yield of hydrocarbon gas increases, while the yield of retained oil is very low, indicating that almost all the oil retained in shale is converted into hydrocarbon gas. It should be noted here that during the hydrocarbon generation simulation experiment, the oil discharged at this stage is mainly the oil discharged from the hydrocarbon generation system, so it does not participate in the evolution process of cracking to gas. Therefore, the oil discharged during the simulation process at this stage is relatively stable. Under geological conditions, it is equivalent that this part of oil has been expelled from the hydrocarbon source series and migrated to the relatively shallow conventional reservoir series.

5 Discussion

5.1 Comparisons of the generation and expulsion efficiency of two different lithological combination shales

Most hydrocarbon generation and expulsion models of lacustrine shale could be divided into four parts (Tang et al., 2018). Similarly, based on the aforementioned experimental simulation results, the evolution of the oil-generating capacity of the source rocks of the Funing Formation in the Subei Basin can be roughly divided into four stages: 1) the source rocks are relatively slow in generating oil, and the hydrocarbon gas generation is very low at this stage; 2) relatively fast oil generation and slow hydrocarbon gas generation stage of the source rock; 3) weak oil generation capacity of the source rock and significantly enhanced hydrocarbon gas generation capacity; and 4) a large amount of oil generation of the source rock to form gas and a large amount of kerogen gas generation stage.

However, the hydrocarbon generation, retention, and expulsion efficiencies of source rocks of different lithological combinations are different. Our experimental results show that the temperature of the pure shale source rock combination is 250–300°C (Ro<0.65%), the residual (retained) oil yield rate is less than 10%, and the residual (retained) amount is greater than 90%; when the temperature is 300–350°C (0.65%<Ro<0.84%), the total oil production rate of the source rock increases rapidly, the oil discharge efficiency increases rapidly, 10%<oil discharge efficiency<75%, and the residual (retained) oil efficiency declines rapidly; when the temperature is about 320°C, the yield of discharged oil is higher than the yield of residual (retained) oil. However, for the shale and thin siltstone combination, when the temperature is 250–335°C (Ro<0.84%), residual (retained) oil production hydrocarbon expulsion efficiency<10% and residual (retained) oil amount>90%; when the temperature is 335–380°C (0.84%<Ro<1.20%), the total oil production rate of the source rock increases rapidly, the oil discharge efficiency increases rapidly, 10%<oil discharge efficiency<75%, and the residual (retained) oil efficiency decreases rapidly; when the temperature is about 360°C, the yield of discharged oil is higher than the yield of residual (retained) oil (Figure 7).

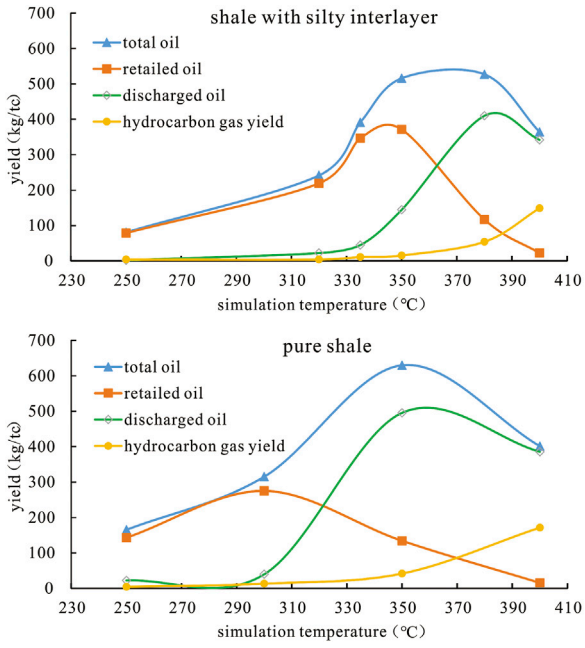

FIGURE 7
Correlation of hydrocarbon generation, expulsion, and retention of different lithological combinations.

Many factors may be involved in hydrocarbon generation, retention, and expulsion between the two lithologies. The very low porosity and permeability of pure thick pure shale allow for high oil retention and weak expulsion, despite its high hydrocarbon capacity (Li et al., 2015; Liang et al., 2017). Brittle minerals also have an effect on oil retention and expulsion. Compared with pure shale, the limestone and siltstone combination has higher carbonate. A large number of organic acids produced during earlier hydrocarbon generation (Ro < 0.84%) dissolve it to form pores, which is conducive to the retention of oil (Hou et al., 2021b). Meanwhile, the siltstone closely adjacent to source rocks provides a channel for the outflow of organic acid-dissolved carbonates, avoids secondary precipitation, and is conducive to the preservation of pores (Li et al., 2018). Pure shale with TOC may generate a large amount of oil rapidly, which may lead to the formation of high pressure in the pores, resulting in the earlier discharge of oils. For the source rocks of shale with more brittle minerals, a large amount of oil can be retained until a certain pressure is formed and then discharged.

Based on the physical models of hydrocarbon generation and expulsion established based on the aforementioned two types of

lithological combinations, combined with the tight oil accumulation conditions of the Funing Formation in the Subei Basin, "discharged oil 1 + discharge oil 2" in the physical model can be regarded as discharged to the neighboring conventional oil in the layer, "discharged oil 3 + discharged oil 4" is regarded as the tight oil discharged into the adjacent layer and the source rock interbedded tight sandstone or carbonate rock, and the rest retained in the source rock shale strata are regarded as retained shale oil in shale.

Therefore, according to this model, the shale oil reservoirs of the Funing Formation in the Subei Basin can be divided into two categories: one is the internal source type, which is discharged into the sandstone or carbonate interlayer within the source rock series to form reservoirs; the other is the source external type in which oil is discharged into the adjacent tight sandstone to form a reservoir or the source rock layer is discharged through faults to form a fault-sand body system to form a reservoir.

5.2 Implications for shale oil exploration in the Subei Basin

The generation and accumulation of shale oil is commonly related to lithofacies (sedimentary environment), maturity (chemical process), and preservation boundary (physical process) (Li et al., 2019). Thermal maturity of source rocks not only controls hydrocarbon generation but also affects the pore system and pressure system, which is a key parameter in the exploration potential of lacustrine shale oil (Zhang et al., 2012). Rui et al. (2020) conducted hydrocarbon generation pyrolysis simulation experiments of the Lucaogou shale and found that the discharge efficiency of hydrocarbons is low during the stage of low maturity of shale, thus proposing that the favorable maturity of shale for shale oil is Ro = 1.0–1.2%. Li et al. (Jarvie, 2012) proposed that at an Ro of 0.84–1.30%, the hydrocarbon expulsion efficiency of lacustrine argillaceous dolomite source rock is the highest, and the discharged oil is mainly accumulated in adjacent sandstone or carbonate reservoirs, which is a favorable maturity range for lacustrine argillaceous dolomite shale oil exploration. However, the previous standards are not recommended to be directly applied to the shale oil exploration of the Funing Formation, and a favorable mature interval should be evaluated considering the geological background.

The hydrocarbon generation and expulsion model of the shale with a silty interlayer combination suggests that at the thermal maturity of Ro =0.84–1.12%, the generated oil is mainly discharged toward adjacent siltstones or carbonate rocks in the formation to form the internal source (Figure 4). For pure shale, oil retention mainly occurs at a maturity of Ro=0.68–0.74, but oil yield is lower in this period. When the maturity is higher than 0.74, the oil yield and oil expulsion efficiency increase rapidly, which indicates that the oil is easy to be filled into the adjacent sandstone along the fault system to form a conventional reservoir, such as a sandstone reservoir in the third member of the Funing Formation (E_1f^3). Most of the E_1f^2 source rocks in the Subei Basin have moderate maturity (Ro = 0.8–1.0%), and the source rocks in the deep depression zone in the Gaoyou Sag and Qingtong Sag can reach Ro = 1.2%. Most of the E_1f^4 source rocks in the Subei Basin have low maturity (Ro = 0.5–0.7%), and the source rocks in the deep depression zone in the Gaoyou Sag, Qintong Sag, and Jinhu Sag can reach high maturity (Ro= 0.7–1.2%) (Fan and Shi, 2019). There are 455 wells in the Subei Basin showing oil and gas in shale, and an obtained industrial oil flow which shows good shale oil exploration prospects (Zan et al., 2021a). Zan et al. (2021a) proposed that the organic-rich silty shale and marlstone with a thermal maturity of Ro >1.1% is divided into favorable area I, the laminated shale and marlstone with a thermal maturity of Ro = 0.9–1.1% is divided into favorable area II, and the massive shale with a thermal maturity of Ro = 0.7–0.9 is divided into favorable area III. Types II and III are mainly composed of shale with a silty interlayer and pure shale, respectively. This classification is consistent with our experimental simulation results. Therefore, the multi-lithology combined shale such as shale with a silty or calcareous interlayer with a thermal maturity of Ro = 0.84–1.12% is suggested to be the favorable maturity range of the Funing Formation, and the deep depression zone with higher thermal maturity (Ro ≈1.1%) in the Sag is a favorable area for shale oil exploration.

6 Conclusion

1) The oil-generation capacity evolution of different lithological combination source rocks in the Funing Formation from the Subei Basin can be roughly divided into four stages: a) relatively slow oil generation and slow gas generation, b) relatively fast oil-generation and slow gas generation, c) oil cracking into gas, and d) kerogen cracking into gas.
2) Different lithological combinations have different oil generation, hydrocarbon expulsion, and retention efficiencies: the total oil generation rate and gas generation rate of pure shale are higher than those of shale with a silty interlayer, and the exchange point between the oil expulsion rate and residual (retention) rate of pure shale is earlier than that of shale with the interlayer. Oil retention mainly occurs when the source rock maturity is Ro=0.84–1.12%, while the discharged oil is mainly accumulated in the adjacent siltstone.
3) Hydrocarbon generation and expulsion models suggest that the favorable maturity of shale oil exploration in the Subei Basin is Ro=0.84–1.12%, the multi-lithofacies combination source rock is the favorable target, and the deep depression zone in the Sag is the favorable area.

Data availability statement

The original contributions presented in the study are included in the article/Supplementary Material; further inquiries can be directed to the corresponding author.

Author contributions

JP: conceptualization and writing—original draft; LL: writing—review and editing, and investigation; CD: visualization; XL: methodology; JZ: project administration; SL: data curation; QQ: formal analysis; and DW: validation and supervision.

Acknowledgments

This research was financially supported by the National Science and Technology Major Project (Nos. 2016ZX05002-006 and 2017ZX05005-003). The editor and two reviewers are acknowledged for providing comments and suggestions which helped improve this manuscript.

Conflict of interest

The authors declare that the research was conducted in the absence of any commercial or financial relationships that could be construed as a potential conflict of interest.

Publisher's note

All claims expressed in this article are solely those of the authors and do not necessarily represent those of their affiliated organizations, or those of the publisher, the editors, and the reviewers. Any product that may be evaluated in this article, or claim that may be made by its manufacturer, is not guaranteed or endorsed by the publisher.

References

Anyiam, O. A., and Onuoha, K. M. (2014). A study of hydrocarbon generation and expulsion of the Nkporo Shales in Anambra Basin, Nigeria. *Arab. J. Geosci.* 7, 3779–3790. doi:10.1007/s12517-013-1064-5

Burnhan, A. K., and Sweeney, J. J. (1989). A chemical kinetic model of vitrinite maturation and reflectance. *Geochem. Cosmochem.* 3, 6–11.

Chai, F. (2019). Study on Paleozoic sedimentary facies and favorable area evaluation in lower Yangtze basin. *Petroleum Reserv. Eval. Dev.* 9 (02), 7–12. doi:10.13809/j.cnki.cn32-1825/te.2019.02.002

Cheng, Q., Zhang, M., and Li, H. (2019). Anomalous distribution of steranes in deep lacustrine facies low maturity-maturity source rocks and oil of Funing formation in Subei Basin. *J. Petroleum Sci. Eng.* 181, 106190. doi:10.1016/j.petrol.2019.106190

Duan, H., Liu, S., and Fu, Q. (2020). Characteristics and sedimentary environment of organic-rich shale in the second member of Paleogene Funing Formation, Subei Basin. *Petroleum Geol. Exp.* 42 (04), 612–617. doi:10.11781/sysydz202004612

Fan, B., and Shi, L. (2019). Deep-lacustrine shale heterogeneity and its impact on hydrocarbon generation, expulsion, and retention: A case study from the upper triassic yanchang formation, Ordos Basin, China. *Nat. Resour. Res.* 28, 241–257. doi:10.1007/s11053-018-9387-2

GB/T 19145-2003 (2003). *Determination of total organic carbon in sedimentary rock*. China: General Administration of Quality Supervision, Inspection and Quarantine of the People's Republic of China.

GB/T 6948-2008 (2008). ISO 7404-5:1994, methods for the petrographic analysis of bituminous coal and anthracite-Part 5: Method of determining microscopically the reflectance of vitrinite, MOD.Standardization administration.

Hill, R. J., Zhang, E., Katz, B. J., and Tang, Y. (2007). Modeling of gas generation from the barnett shale, fort worth basin, Texas. *Am. Assoc. Pet. Geol. Bull.* 91 (4), 501–521. doi:10.1306/12060606063

Hou, L., Luo, X., Lin, S., Zhao, Z., and Li, Y. (2021). Quantitative Measurement of Retained Oil in Organic-Rich Shale—A Case Study on the Chang 7 Member in the Ordos Basin, China. *Front. Earth Sci.* 9, 662586. doi:10.3389/FEART.2021.662586

Hou, L., Ma, W., Luo, X., Liu, J., Liu, S., and Zhao, Z. (2021). Hydrocarbon generation-retention-expulsion mechanism and shale oil producibility of the permian lucaogou shale in the Junggar Basin as simulated by semi-open pyrolysis experiments. *Mar. Petroleum Geol.* 125, 104880. doi:10.1016/J.MARPETGEO.2020.104880

Hu, T., Pang, X., Jiang, S., Wang, Q., Zheng, X., Ding, X., et al. (2018). Oil content evaluation of lacustrine organic-rich shale with strong heterogeneity: A case study of the middle permian lucaogou Formation in jimusaer sag, Junggar Basin, NW China. *Fuel* 221, 196–205. doi:10.1016/j.fuel.2018.02.082

Hu, T., Pang, X., Jiang, S., Wang, Q., Liu, X., Wang, Z., et al. (2021). Movable oil content evaluation of lacustrine organic-rich shales: Methods and a novel quantitative evaluation model. *Earth-Science Rev.* 214, 103545. doi:10.1016/J.EARSCIREV.2021.103545

Hu, T., Wu, G., Xu, Z., Pang, X., Liu, Y., and Yu, S.(2022). Potential resources of conventional, tight, and shale oil and gas from Paleogene Wenchang Formation source rocks in the Huizhou Depression. *Adv. Geo-Energy Res.*6(5), 402–414. doi:10.46690/ager.2022.05.05

Jarvie, D. M. (2012). Shale resource systems for oil and gas: Part 2: shale-oil resource systems. *AAPG Mem.* 97, 89–119. doi:10.1306/13321447M973489

Ji, Y., Liu, Y., and Feng, W. (2013). Source rock study and accumulation pattern of Funing Formation in Yancheng sag, northern Jiangsu basin. *Petroleum Geol. Exp.* 35 (4), 449–452. doi:10.11781/sysydz201304449

Jia, C., Zou, C., Li, J., Li, D., and Zheng, M. (2012). Assesment criteria, main types, basic features and resource prospects of the tight oil in China. *Acta Pet. Sin.* 33 (3), 333–350. doi:10.7623/syxb201203001

Jia, W., Wang, Q., Liu, J., Peng, P., Li, B., and Lu, J. (2014). The effect of oil expulsion or retention on further thermal degradation of kerogen at the high maturity stage: A pyrolysis study of type II kerogen from pingliang shale, China. *Org. Geochem.* 71, 17–29. doi:10.1016/j.orggeochem.2014.03.009

Jin, Z., Zhu, R., Liang, X., and Shen, Y. (2021). Several issues worthy of attention in current lacustrine shale oil exploration and development. *Petroleum Explor. Dev.* 48 (6), 1471–1484. doi:10.1016/s1876-3804(21)60303-8

Li, J., Wang, W., Cao, Q., Shi, Y., Yan, X., and Tian, S. (2015). Impact of hydrocarbon expulsion efficiency of continental shale upon shale oil accumulations in eastern China. *Mar. Petroleum Geol.* 59, 467–479. doi:10.1016/j.marpetgeo.2014.10.002

Li, Z., Zheng, L., Jiang, Q., Ma, Z., Tao, G., Xu, E., et al. (2018). Simulation of Hydrocarbon generation and expulsion for lacustrine organic-rich argillaceous dolomite and its implications for shale oil exploration. *Earth Sci.* 43 (2), 566–576. doi:10.3799/dqkx.2018.025

Li, M., Jin, Z., Dong, M., Ma, X., Li, Z., Jiang, Q., et al. (2019). Advances in the basic study of lacustrine shale evolution and shale oil accumulation. *Petroleum Geol. Exp.* 42 (4), 489–505. doi:10.11781/sysydz202004489

Liang, C., Cao, Y., Jiang, Z., Wu, J., Song, G., and Wang, Y. (2017). Shale oil potential of lacustrine black shale in the eocene dongying depression: implications for geochemistry and reservoir characteristics. *Am. Assoc. Pet. Geol. Bull.* 101 (11), 1835–1858. doi:10.1306/01251715249

Liu, X., Lai, J., Fan, X., Shu, H., Wang, X., Shu, H., et al. (2020). Insights in the pore structure, fluid mobility and oiliness in oil shales of Paleogene Funing Formation in Subei Basin, China. *Mar. Petroleum Geol.* 114, 104228. doi:10.1016/j.marpetgeo.2020.104228

Liu, D. (2010). Analysis on structural evolution of northern jiangsu-south Yellow Sea basin. *J. Oil Technol.* 32 (6), 27–31. doi:10.3969/j.issn.1000-9752.2010.06.006

Liu, L. (2019). *Recovery of paleopressure and paleo-fluid potential of Funing Formation in Gaoyou sag*. Beijing: China University of petroleum.

Lu, S., Wang, M., Wang, Y., Xu, L., Xue, H., and Li, J. (2006). Comparison of simulation results from the closed and open experimental system and its significance. *Acta Sedimentol. Sin.* 24 (2), 282–288.

Ma, Z., Zheng, L., Xu, X., Bao, F., and Yu, X. (2017). Thermal simulation experiment of organic matter -rich shale and implication for organic pore formation and evolution. *Petroleum Res.* 2 (4), 347–354. doi:10.1016/j.ptlrs.2017.04.005

Ma, W., Hou, L., Luo, X., Liu, J., Tao, S., Guan, P., et al. (2020). Generation and expulsion process of the Chang 7 oil shale in the Ordos Basin based on temperature-based semi-open pyrolysis: Implications for *in-situ* conversion process. *J. Petroleum Sci. Eng.* 190, 107035. doi:10.1016/j.petrol.2020.107035

Ma, Z., Tan, J., Zheng, L., Shen, B., Wang, Z., Shahzad, A., et al. (2021). Evaluating gas generation and preservation of the Wufeng-Longmaxi Formation shale in southeastern Sichuan Basin, China: Implications from semi-closed hydrous pyrolysis. *Mar. Petroleum Geol.* 129, 105102–105112. doi:10.1016/J.MARPETGEO.2021.105102

Mahlstedt, N., and Horsfield, B. (2012). Metagenetic methane generation in gas shales I. Screening protocols using immature samples. *Mar. Petroleum Geol.* 31 (1), 27–42. doi:10.1016/j.marpetgeo.2011.06.011

Mukhopadhyay, P. K., Wade, J. A., and Kruge, M. A. (1995). Organic facies and maturation of Jurassic/Cretaceous rocks, and possible oil-source rock correlation based on pyrolysis of asphaltenes, Scotian Basin, Canada. *Org. Geochem.* 22 (1), 85–104. doi:10.1016/0146-6380(95)90010-1

Peng, J., Qi, Q., Wang, D., Li, Z., Zhu, J., Liang, S., et al. (2020). Occurrence and recoverability of tight oil in Paleogene Funing Formation, Subei Basin. *Petroleum Geol. Exp.* 42 (1), 53–59. doi:10.11781/sysydz202001053

Qi, K., Zhao, X., Liu, L., Su, Y., Wang, H., Tan, C., et al. (2018). Hierarchy and subsurface correlation of muddy baffles in lacustrine delta fronts: a case study in the X oilfield, Subei Basin, China. *Pet. Sci.* 15, 451–467. doi:10.1007/s12182-018-0239-9

Qin, L., Zhang, Z., Zhu, L., Liu, H., and Xi, W. (2011). Productions of closed system experiments for middle permian source rock in southern Junggar Basin. *Nat. Gas. Geosci.* 22 (5), 860–865. doi:10.11764/j.issn.1672-1926.2011.05.860

Quaye, J., Jiang, Z., and Zhou, X. (2018). Bioturbation influence on reservoir rock quality: A case study of well bian-5 from the second member paleocene Funing Formation in the Jinhu sag, Subei basin, China. *J. Petroleum Sci. Eng.* 172, 1165–1173. doi:10.1016/j.petrol.2018.09.026

Rui, X., Zhou, Y., Li, Z., and Zhang, Q. (2020). Characteristics of source rocks and reservoirs of the Funing Formation in the Subei Basin and their bearing on future shale oil exploration. *Mar. Geol. Quat. Geol.* 40 (6), 133–145. doi:10.16562/j.cnki.0256-1492.2020010301

Shi, C., Cao, J., Tan, X., Luo, B., Zeng, W., Hong, H., et al. (2018). Hydrocarbon generation capability of Sinian–Lower Cambrian shale, mudstone, and carbonate rocks in the Sichuan Basin, southwestern China: Implications for contributions to the giant Sinian Dengying natural gas accumulation. *Am. Assoc. Pet. Geol. Bull.* 102, 817–853. doi:10.1306/0711171417417019

Shi, S. (2010). Characteristics and spatial distribution of the mesozoic-paleozoic strata in the Yanfu area, north Jiangsu. *J. Stratigr.* 34 (01), 106–111.

Shu, L., Wang, B., Wang, L., and He, G. (2005). Analysis of northern Jiangsu prototype basin from late cretaceous to neogene. *Geol. J. China Univeristies* 04, 534–543. doi:10.3969/j.issn.1006-7493.2005.04.009

Tang, X., Zhang, J., Jiang, Z., Zhao, X., Liu, K., Zhang, R., et al. (2015). Characteristics of solid residue, expelled and retained hydrocarbons of lacustrine marlstone based on semi-closed system hydrous pyrolysis: Implications for tight oil exploration. *Fuel* 162, 186–193. doi:10.1016/j.fuel.2015.09.009

Tang, X., Zhang, J., Jiang, Z., Zhang, R., Lan, C., Zhao, W., et al. (2018). Heterogeneity of organic-rich lacustrine marlstone succession and their controls to petroleum expulsion, retention, and migration: A case study in the shulu sag, bohai bay basin, China. *Mar. Petroleum Geol.* 96, 166–178. doi:10.1016/j.marpetgeo.2018.05.031

Uguna, C. N., Carr, A. D., Snape, C. E., and Meredith, W. (2016). Retardation of oil cracking to gas and pressure induced combination reactions to account for viscous oil in deep petroleum basins: Evidence from oil and n -hexadecane pyrolysis at water pressures up to 900bar. *Org. Geochem.* 97, 61–73. doi:10.1016/j.orggeochem.2016.04.007

Wang, X., Liang, Q., Gao, C., Xue, P., Yin, J., and Hao, S. (2022). Hydrocarbon accumulation model influenced by"three elements (source-storage-preservation)"in lacustrine shale reservoir-A case study of Chang 7 shale in Yan'an area, Ordos Basin. *Front. Earth Sci.* 10. doi:10.3389/feart.2022.1012607

Yang, H., Liang, X., Niu, X., Feng, S., and You, Y. (2017). Geological conditions for continental tight oil formation and the main controlling factors for the enrichment: A case of Chang 7 member, triassic yanchang formation, Ordos Basin, NW China. *Petroleum Explor. Dev.* 44 (1), 11–19. doi:10.1016/s1876-3804(17)30003-4

Yao, H., Zan, L., Gao, Y., Hua, C., Yu, W., Luo, W., et al. (2021). Main controlling factors for the enrichment of shale oil and significant discovery in second member of Paleogene Funing Formation, Qintong Sag, Subei Basin. *Petroleum Geol. Exp.* 43 (5), 776–783. doi:10.11781/sysydz202105776

Zan, L., Luo, W., Yin, Y., and Jing, X. (2021). Formation conditions of shale oil and favorable targets in the second member of Paleogene Funing Formation in Qingtong sag, Subei Basin. *Petroleum Geol. Exp.* 43 (2), 233–241. doi:10.11781/sysydz202102233

Zan, L., Chai, F., and Yin, Y. (2021). Physical properties, geochemical characteristics and origins of crude oils in the QintongSag slope. *Acta Sedimentol. Sin.* 39 (5), 1068–1077. doi:10.14027/j.issn.1000-0550.2020.088

Zhang, J., Liu, B., Mao, F., and Chang, X. (2003). Clastic diagenesis and reservoir characteristics of Funing formation in north slope of Gaoyou Depression in Subei Basin. *Acta Pet. Sin.* 24 (2), 43–49. doi:10.3321/j.issn:0253-2697.2003.02.009

Zhang, J., Lin, L., Li, Y., Tang, X., Zhu, L., Xing, Y., et al. (2012). Classification and evaluation of shale oil. *Geosci. Front.* 19 (05), 322–321.

Zhao, S., Fu, Q., Luo, W., Huang, J., and Teng, J. (2022). The hydrocarbon accumulation regularity and the model of hydrocarbon accumulation along the fault ridges in the slope zone of the continental fault basin. *J. Petroleum Sci. Eng.* 208, 109188. doi:10.1016/j.petrol.2021.109188

Zheng, L., Qin, J., He, S., Li, G., and Li, Z. (2009). Preliminary study of formation porosity thermocompression simulation experiment of hydrocarbon generation and expulsion. *Petroleum Geol. Exp.* 31 (3), 296–302. doi:10.3969/j.issn.1001-6112.2009.03.017